ISSN 1330-3651 (Print), ISSN 1848-6339 (Online) https://doi.org/10.17559/TV-20231227001236
Original scientific paper

Efficient MIMO Antenna Design Using Metamaterials for Compact and High-Performance Communication Applications

R. SUDHA*, S. BHAVANI

Abstract: The proposed metamaterial-based MIMO antenna has four individual elements, each of which is fed by a microstrip feed. The total width and length of the structure are respectively 60 and 52 millimetres. The metamaterial is dispersed from the fields with the strongest coupling by being printed on a patch. This makes the isolation better. The distributions of the fields are altered as a result of the electromagnetic fields' interactions with the metamaterial structure, which reduces the number of coupled fields. The suggested antenna design is the simplest and takes up the least amount of area because metamaterials are produced as patches. The proposed architecture's strong impedance bandwidth operates at 18.3 GHz, 10.8 GHz, 12.3GHz, 13.7 GHz, 16.1 GHz, 18.1 GHz. The suggested structure has all four ports of excitation, a gain of greater than 6.dBi on all operating bands, and a broadside radiation pattern. Tolerable levels of error (ECC and CCL) are achieved in their respective operational bands. A prototype of the proposed antenna is then constructed and evaluated. Because the simulated value and the measured value are so close to one another, MIMO is the most efficient form of wireless transmission.

Keywords: broadside radiation pattern; impedance bandwidth; metamaterial-based design; MIMO antenna; wireless transmission efficiency

1 INTRODUCTION

High data transfer speeds and low bit error probability are two criteria that the next generation of wireless communication networks must satisfy. Most research in this area focuses on how to improve wireless network performance by deploying cutting-edge infrastructure. It is generally agreed that using multiple input multiple output (MIMO) antennas is a great way to boost transmission dependability [1]. Multiplexing gains, variety gains, fewer occurrences of multiple fading events, and increased channel capacity all contribute to this goal. Multiple-input multiple-output (MIMO) technology is widely acknowledged as a crucial component of current and future wireless data communications standards, including 3G, 4G, and shortly 5G networks. As isolation between antenna parts has such a significant impact on wireless channels, diversity performance, and channel capacity, it is the most important aspect of constructing a MIMO system. MIMO antennas limit mutual coupling to 12 dB [2]. Careful pre-construction planning does this. Many methods have been proposed to reduce mutual coupling between antennas, such as using a dielectric substrate with a high permittivity [3]. Microstrip antennas have also been shrunk. Antenna mutual coupling has been reduced using many approaches. Defective ground structures (DGS) on the ground plane can greatly minimise port mutual coupling [4-9]. To rephrase, MIMO antenna performance can be enhanced while isolation is also improved by employing an electromagnetic band gap (EBG) structure [10, 12]. According to the research published in [13], a meta-material structure is used in a MIMO antenna to improve its isolation. Many x-band MIMO antennas that were created using various approaches are mentioned in [14-16]. In modern communication systems, the use of sizable dish antennas in radar and satellite applications is gradually being replaced by more compact and streamlined alternatives. Traditional satellite antennas operating at ultra-high frequency or very high frequency require larger dimensions as wavelengths lengthen. On the contrary, satellite antennas operating within the Ku/K band offer compactness, lower initial investment requirements, improved cost-effectiveness, and increased reliability. These antennas find utility not only in individual satellites but also in satellite constellations, diverse wireless communication scenarios, and educational contexts. By a series of experiments and one-of-a-kind technologies, it was possible to develop MIMO antennas that were miniature, low in size, and had low envelope correlation coefficients. ISM (2.4 GHz) mobile phones can now benefit from Sun and Wei's [17, 18] creation of a 4 × 4 MIMO antenna system. Using periodic split ring resonators (SRRs) on the metasurface is the MAAD Method for Mutual Coupling Reduction in a MIMO Antenna System [19]. This method is also known as the Antenna Array Decoupling (MAAD) Method. A complementing split ring resonator structure makes the patch pentaband MIMO antenna small and isolated. The antenna may utilise K band frequencies for satellite communications. Back-to-back symmetrical antenna elements with orthogonal polarisation reduce mutual contact. This reduces building size. There is a connection made between a microstrip feed that has a characteristic impedance of 50 ohms and a DMS that has been cut into the top octagonal patch and has a width of one millimetre. In order to provide a more seamless transition across frequency ranges, the ground plane's height was reduced. As a result, we investigate and analyse the features of the MIMO antenna, which include its radiation patterns, envelope correlation coefficient, diversity gain, and reflection coefficient S11. The envisioned building is created with the help of a substrate made of FR-4, which can be purchased at a reasonable price. It also features excellent impedance matching, robust isolation, and a compact size, which are all advantages. In addition to having a straightforward layout, its construction is uncomplicated and straightforward. The suggested antenna is shown in both its single and MIMO variants in Fig. 1, which may be found below.

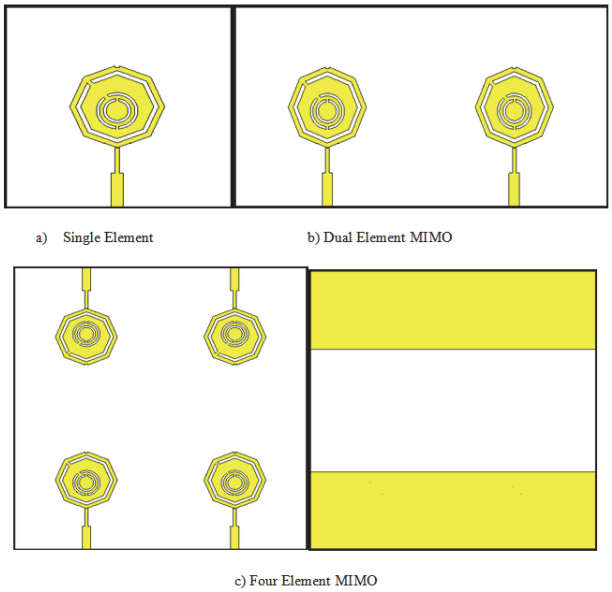

Figure 1 Different stages of proposed antenna

2 ANTENNA GEOMETRY

The proposed construction, which includes a micro-strip feed line, is mounted on a 1.6 millimetre-thick FR-4 substrate with a dielectric constant of 4.4 and a loss tangent of 0.02. Substrate dielectric constant is 4.4, loss tangent is 0.02. These values are listed below. Four CSRR-carved octagonal patches make up the proposed MIMO antenna.These components are comparable to one another. The top layer of the substrate has matching orthogonal micro-strip lines, which are used to provide power to these elements after they have been placed back-to-back. The suggested antenna's individual component is shown in Fig. 2, which may be seen here. On substituting the values fr = 8 GHz & ε_r = 4.4 , F= 0.5238. Substituting F = 0.5238 & h = 0.0016, a = 5.879 mm, ae = 5.98mm.

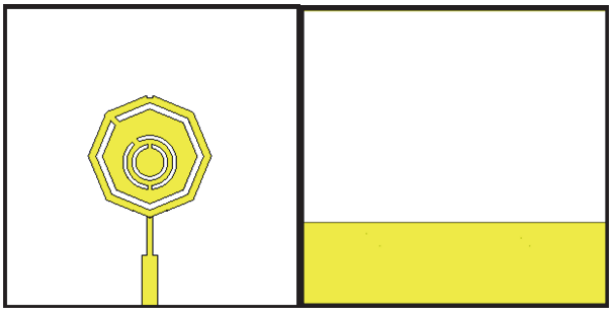

Figure 2 Single Element

The suggested antenna has a straightforward patch in the shape of an octa, and it will operate at a frequency of 10 GHz. After that, the impedance is matched by including the decreased ground plane into the circuit. The patch construction is carved with numerous Complementary Split Ring resonators so that the antenna can operate across many frequency bands. More resonance is produced as a result of the engraving of three CSRRs onto the patch. Fig. 3 illustrates the various dimensions of the antenna.

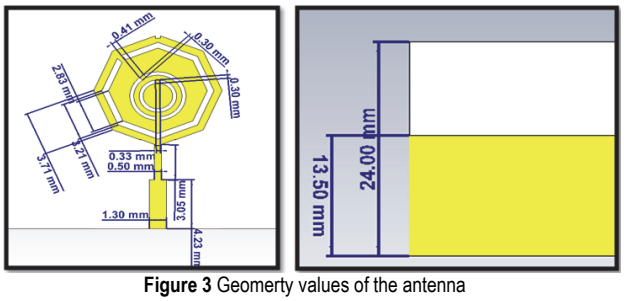

Figure 3 Geomerty values of the antenna

2.1 Design Evolution

Antenna A is a microstrip feed antenna that has a straightforward octal design and a very low impedance bandwidth. Antenna B is a modified version of antenna A that functions at three different bands using CSRR. It employs a patch that has circular metamaterial forms carved into it to provide this functionality. The design of antenna C allows it to function in three bands while maintaining a higher bandwidth thanks to the octa-shaped CSRR that was etched into it. The last choice is Antenna D, which consists of four elements and may function in a total of six bands. In Fig. 4, a comparison is made between the return loss plots of the first three stages. Fig. 5 presents the completed MIMO transmission and reflection antenna array for a 4 × 4 configuration.

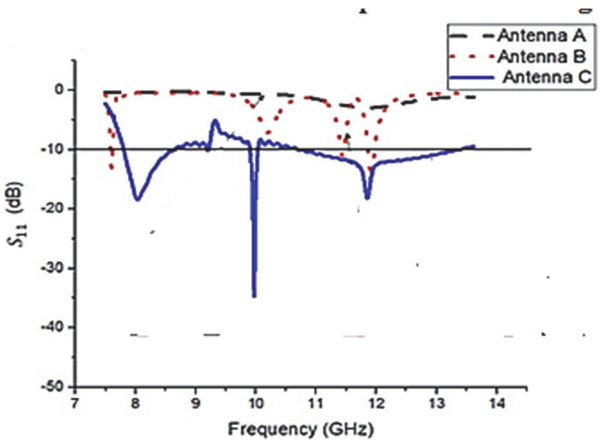

Figure 4 S11 comparison plot of the first three evolution stage

Due to the fact that it is a straightforward octa-shaped microstrip feed antenna with the full ground, Antenna A is incapable of satisfying the impedance criteria. The following is a list of frequency ranges that are covered by the circular CSRR etch that is utilised for antenna B: 7.71 to 7.79 GHz, 11.81 to 11.83 GHz, and 11.89 to 12.01 GHz are the ranges that this frequency covers. The CSRR's Antenna C has eight different facets, and its frequency ranges for each of its three bands are as follows: 7.83 GHz to 8.52 GHz, 9.91 GHz to 10.01 GHz, and 11.21 GHz to 13.84 GHz. MIMO antenna consists of six bands that operate at frequencies ranging from 8.26 GHz to 8.53 GHz, 10.72 GHz to 11.01 GHz, 12.21 GHz to 12.51 GHz, 13.41 GHz to 14.17 GHz, 15.8 GHz to 16.02 GHz, and 17.93 GHz to 18.33 GHz respectively.

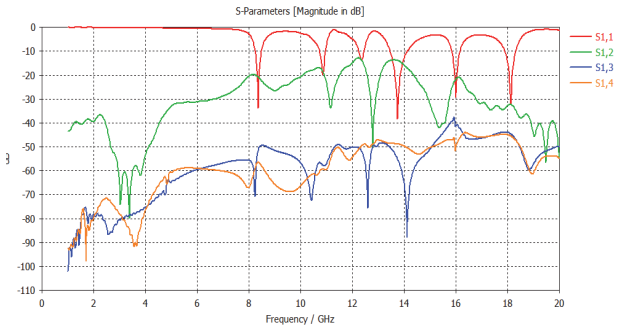

Figure 5 Reflection and transmission plot of the 4 x 4 MIMO antenna

2.2 Four x Four MIMO Design

One technique to expand channel capacity and improve communication quality without incurring additional expenditures in terms of radiation power or spectrum bandwidth is to increase the number of transmitting and receiving antennas. This can be done by increasing the number of antennas that are used for both sending and receiving signals. This is due to the fact that increasing the number of antennas used for broadcasting and receiving does not result in any additional costs being incurred. In this section of the article, it is shown that there are four symmetrical ground elements printed on the lower face of the substrate, in addition to four symmetrical monopole antenna elements printed on the upper face of the substrate. These components are designed to be utilised in contexts requiring satellite-band operation. Throughout its entirety, this component has a total square measurement of 48 millimetres by 46 millimetres. A 50 - microstrip line supplies electrical current to each element of the antenna so that it can be powered by the antenna itself. A visual illustration of the space-saving configuration of a quad-element MIMO antenna is presented in Fig. 6, which was mentioned earlier and is supplied there. Fig. 7 provides a visual representation of the voltage standing wave ratio (VSWR) of the antenna.

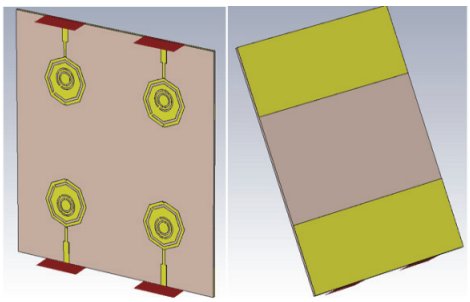

Figure 6 MIMO antenna at CST environment

The simulated S-parameters of the proposed four-element MIMO antenna are shown as a function of frequency in Fig. 7, which is a representation of those results. The figure provides an illustration of this representation. The S-parameter may be simply analysed by taking into mind the equations S11 = S22 = S33 = S44, S21 = S12 = S34 = S43, S13 = S31 = S42 = S24, and S14 = S41 = S23 = S32. This is because symmetry makes it easy to evaluate the S-parameter. The table that follows contains these equations for your convenience. At the operating frequency band, the isolation between port 1 and port 2/port 3, as demonstrated by |S12| and |S13|, is extremely high and is greater than 20 dB and 40 dB, respectively. Since the proposed antenna has a minimum isolation of roughly 40 dB between ports 1 and 4, it has been proved that the quad-element MIMO antenna has a good performance, which was demonstrated by the fact that it has an exceptional performance.

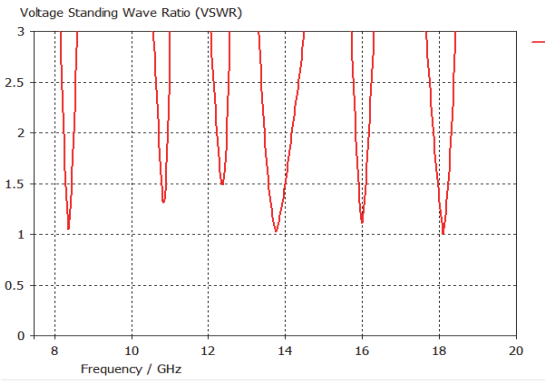

Figure 7 VSWR of the 4 x 4 MIMO antenna

3 ANTENNA PERFORMANCE

To clean a copper-clad FR4 substrate that has been etched on both sides, acetone is utilised as the solvent of choice. Following the completion of the drying process for the photoresist film, the structure is then laminated with the film. After that, the mask, which is the opposite of the pattern that is required, is glued to the photoresist laminated FR4 substrate, and then UV light is shone on it. After that, the substrate is dissolved in a developer solution that contains sodium carbonate, and then a ferric chloride solution is used to etch it. After that, sodium hydroxide is applied to the region so that the hardened photoresist may be dissolved and the desired antenna can be developed. Fig. 8 illustrates the antenna that was manufactured, and Fig. 9 illustrates the impact that the ground plane had on the return loss plot. Fig. 10 demonstrates very plainly that the decreased size of the ground plane has a far higher impact on the impedance bandwidth of the proposed antenna.

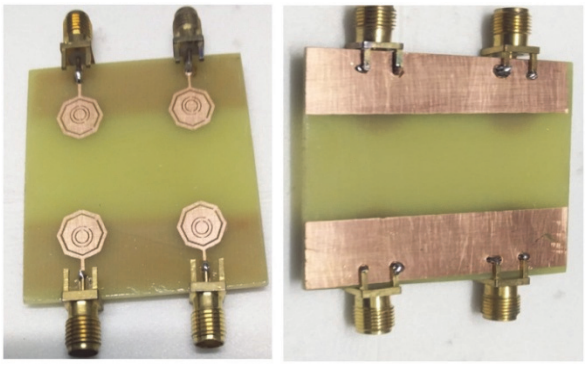

Figure 8 Fabricated Antenna

Fig. 10, which can be seen further down on this page, is an illustration of the surface current density that the suggested antenna has. We are able to get to the conclusion that the coupling fields that are present between the elements are significantly reduced as a result of the presence of the metamaterial structure because of the fact that this is something that is present. It is not impossible for

the structure of the metamaterial to detach the most substantial coupling field that now exists between the elements; this is something that is plausible. As a direct result of this, the isolation will be significantly strengthened.

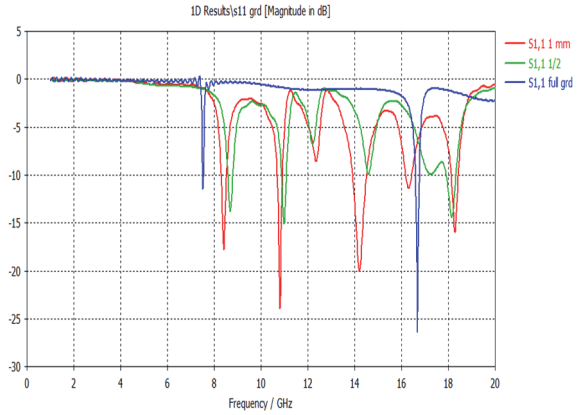

Figure 9 Effect of ground

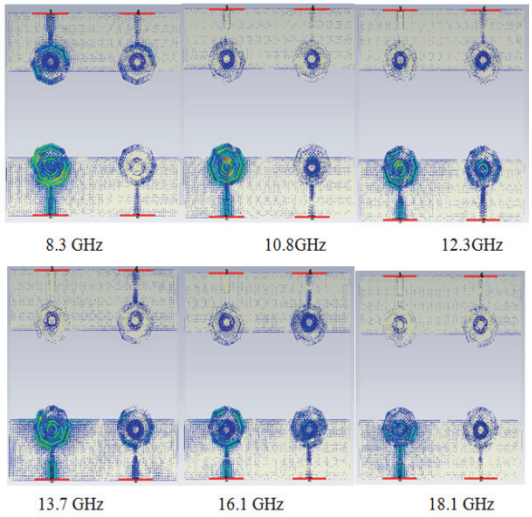

Figure 10 Surface current distribution at various resonant frequencies

Fig. 11 depicts the radiation pattern that the proposed antenna would emit in a number of resonant bands in the event that it was built. This pattern would be visible in the event that the proposed antenna was built. The 3D radiation pattern is depicted as the patterns for the E and H planes in Fig. 11, which may be found here. MATLAB was used to make this particular figure. The radiation pattern demonstrates a continuous omnidirectional pattern, which is a crucial need for any communication application. The pattern can be seen here. The reason for this is that electromagnetic waves have the feature of being able to travel in any direction. This is due to the fact that the omnidirectional pattern has the potential to extend in any direction. Because the structure of the metamaterial is printed on the patch, which is situated in an area with a weak electric field, the radiation pattern is not significantly altered by the structure of the metamaterial. This is due to the fact that the patch is located in an area with a weak electric field. As a consequence of this, the pattern of the radiation has seen very little discernible change. The H plane generates an omnidirectional pattern, whereas the E lane generates a dipole in the shape of an 8. The omnidirectional pattern is generated by the H plane.ž

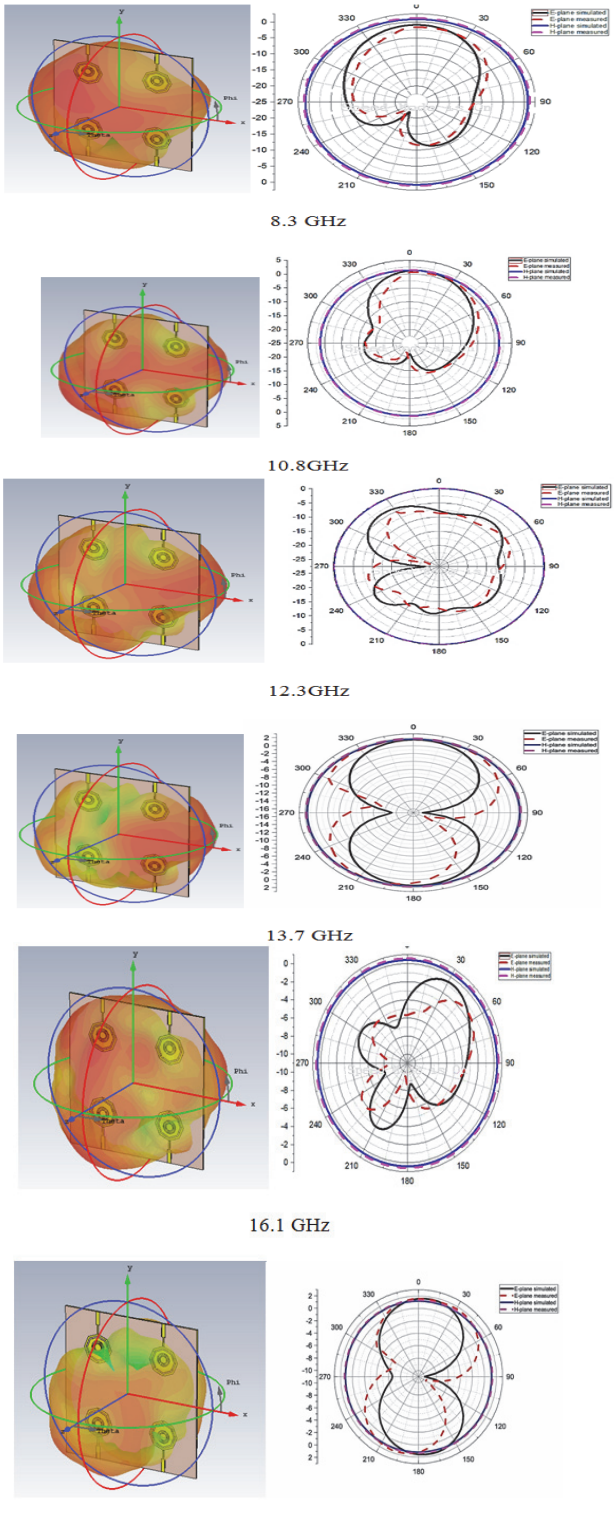

Figure 11 3D Radiation pattent , E plane and H plane (Measured Vs. Simulated) various resonant frequencies

Tab. 1 presents the results of an evaluation that compares the proposed MIMO to a number of antennas that were used in the relevant study. The gain is displayed against the frequency in Fig. 13, which may be seen below. The gains of a single element and a MIMO configuration are plotted, and it can be seen very clearly that the MIMO design results in a greater gain.

Table 1 Comparison of the proposed antenna with literature

Ref	Operating frequency	Elements	Operating bands	Gain
20	2.4, 3.5, 5.5	2	3	3.2
21	4.75, 5.89, 6.74, 8.25, 9.82	2	5	NA
22	2.6, 3.5, 5. 2	4	3	NA
23	2.25, 2.6, 5.2, 24, 28	4	5	5
24	3.5, 4.8, 5.5	8	3	4.8
25	3.5, 5.2	2	2	4.7
26	5.3	4	1	3
27	5.8	4	1	4.1
28	5.7	4	1	4
Proposed	8.3, 10.8, 12.3, 13.7, 16.1, 17.1	4	6	6.5

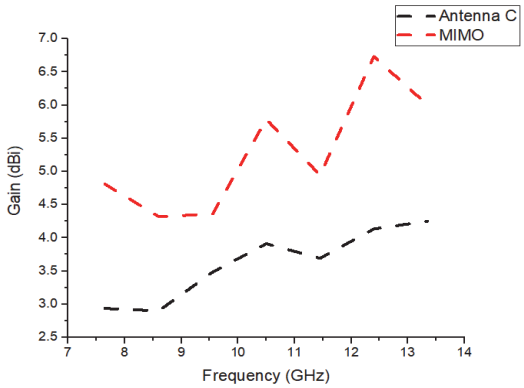

Figure 12 Gain (MIMO Vs Single Element)

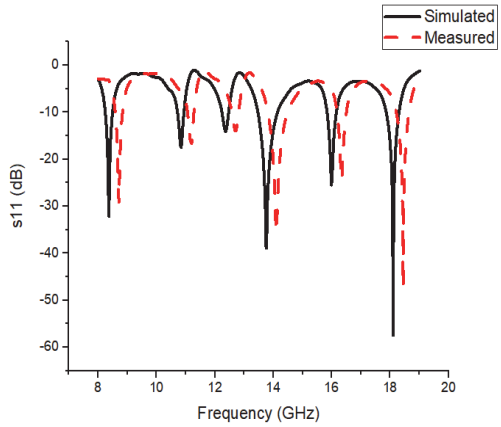

Figure 13 Simulated Vs. measured S11

Fig. 13 depicts a comparison between the simulated and measured return loss; the differences are the result of fabrication and measurement errors, respectively. Using the antenna diversity parameter as a basis for one's assessment of the antenna's MIMO performance is one way to go about doing so. One of these three distinct kinds of strategies can be utilised to bring about the desired effect of diversity. 1) the variety of space that is available; 2) the variety of polarisations that are feasible; and 3) the variety of patterning that is achievable. In order to realise the antenna diversity and to raise the isolation between two closely coupled antennas, this study adopts a method that is known as spatial diversity. Moreover, the isolation between the two antennas that are tightly coupled has been strengthened. It is possible to quantify the isolation between two tightly linked antennas by utilising either the far field pattern or the s parameter. However, the ECC is used to obtain this measurement because of its higher level of precision. It is generally agreed upon that when the value of the ECC is relatively low, the performance of the MIMO antenna diversity is high. In a multiple input multiple output (MIMO) antenna system, you will be able to calculate the envelope correlation coefficient that exists between antennas i and j by making use of the formulas that are presented further down in this section.

$$\rho_e(\mathrm{i},\mathrm{j},\mathrm{N}) = \left| \frac{\sum_{n=1}^{N} S_{i,n}^{*} S_{n,j}}{\Pi_{k=i,j}\left(1-\sum_{n=1}^{N} S_{k,n}^{*} S_{n,j}\right)} \right| \quad (1)$$

For Two element MIMO:

$$\rho_e(1,2,2) = \frac{\left|S_{11}^{*}S_{12} + S_{21}^{*}S_{22}\right|}{\left(1-\left|S_{11}\right|^2-\left|S_{21}\right|^2\right)\left(1-\left|S_{22}\right|^2-\left|S_{11}\right|^2\right)} \quad (2)$$

It is demonstrated through the use of the simulated envelope correlation coefficient that the ECC value is significantly lower than 0.05 for the entirety of the operational spectrum. This conclusion cannot be disputed. The following equation was utilised in order to ascertain the amount of diversity gain that was accomplished. $DG = 10\ p$, $p = (1–|0.99e|2)1/2$; where 10 is the maximum DG with the selection combining probability level of 1% an approximate equation for correlation efficiency.

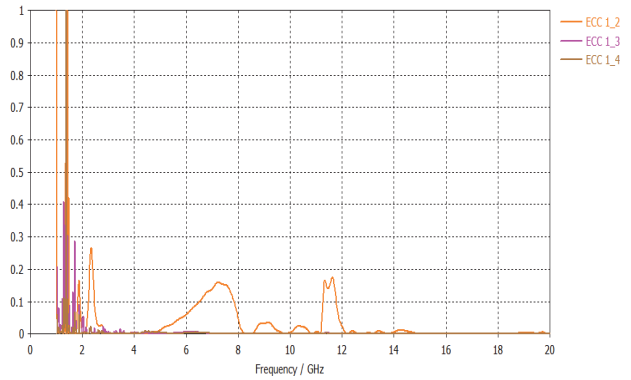

Figure 14 ECC Plot Vs Frequency

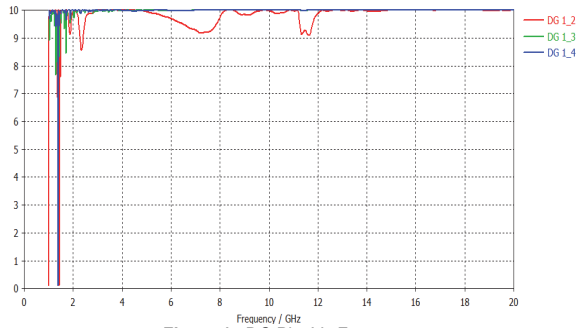

Figure 15 DG Plot Vs Frequency

4 CONCLUSION

For satellite communications, we provide a 4 × 4 metamaterial MIMO antenna. It is built on a 46 mm × 48 mm FR4 substrate. Printed patch resonators are powered by a microstrip feed. At its resonant frequencies of 8.26 - 8.53 GHz, 10.72 - 11.01 GHz,

12.21 - 12.51 GHz, 13.41 - 14.17 GHz, 15.8 - 16.02 GHz, and 17.93 - 18.33 GHz, this structure offers isolation better than –20 dB. This seclusion is further improved by a unique metamaterial structure that is printed onto the patch. The patch includes this structure. Metamaterial features on the antenna's low-field portion decouple fields between tightly coupled antenna elements without changing radiation pattern. Metamaterials improve isolation, the most crucial MIMO parameter. CST built and displayed all simulated outcomes. Due to its low ECC value, steady radiation pattern, and high gain, the provided MIMO antenna is the best choice for future wireless communication.

6 REFERENCES

[1] Xu, H., Zhijiao, C., Haiwen, L., Le, C., Taotao, H., Sheng, Y., Lina, Z., & Chao D. (2022). Single-fed dual-circularly polarized stacked dielectric resonator antenna for K/Ka-band UAV satellite communications. *IEEE Transactions on Vehicular Technology, 71*(4), 4449-4453. https://doi.org/10.1109/TVT.2022.3144414

[2] Ahmed, B. T., Olivares, P. S., Campos, J. L. M., & V´azquez, F. M. (2018). 3.1 - 20 GHz MIMO antennas. *AEU - International Journal of Electronics and Communications, 94*, 348-358. https://doi.org/10.1016/j.aeue.2018.07.026

[3] Roja, G., Maheswara Venkatesh, P., & Jayasankar, T. (2023). Split Ring Resonator Inspired Dual-Band Monopole Antenna for ISM, WLAN, WIFI, and WiMAX Application. *Technical Gazette, 30*(5), 1533-1538. https://doi.org/10.17559/TV-20230210000344

[4] Yang, B., Chen, M., & Li, L. (2018). Design of a four-element WLAN/LTE/UWB MIMO antenna using half-slot structure. *International Journal of Electronics and Communications, 93*, 354-359. https://doi.org/10.1016/j.aeue.2018.05.034

[5] Acharjee, J., Mandal, K., & Mandal, S. K. (2018). Reduction of mutual coupling and cross-polarization of a MIMO/diversity antenna using a String of H-shaped DGS. *AEU - International Journal of Electronics and Communications, 97*, 110-119. https://doi.org/10.1016/j.aeue.2018.09.037

[6] Manouare, A. Z., Ibnyaich, S., El Idrissi, A., & Ghammaz, A. (2016). Miniaturized triple wideband CPWfed patch antenna with a defected ground structure for WLAN/WiMAX applications. *Journal of Microwaves, Ptoelectronics and Electromagnetic Applications, 15*(3), 157-169. https://doi.org/10.1590/2179-10742016v15i3497

[7] Banerjee, J., Karmakar, A., Ghatak, R., & Poddar, D. R. (2017). Compact CPW-fed UWB MIMO antenna with a novel modified Minkowski fractal Defected Ground Structure (DGS) for high isolation and triple bandnotch characteristic. *Journal of Electromagnetic Waves and Applications, 31*(15), 1550-1565. https://doi.org/10.1080/09205071.2017.1354727

[8] Kamal, S. & Chaudhari, A. A. (2017). Printed meander line MIMO antenna integrated with air gap, DGS and RIS: A low mutual coupling design for LTE applications. *Progress in Electromagnetics Research C, 71*, 149-159. https://doi.org/10.2528/PIERC16112008

[9] Bhadouria, A. S. & Kumar, M. (2014). Microstrip X-band antenna with improvement in performance using DGS. *Electrical and Electronic Engineering, 4*(2), 31-35.

[10] Kumar, N. & Kommuri, U. K. (2018). MIMO antenna mutual coupling reduction for WLAN using spiro meander line UC-EBG. *Progress in Electromagnetics Research C, 80*, 65-77. https://doi.org/10.2528/PIERC17101601

[11] Dabas, T., Gangwar, D., Kanaujia, B. K., & Gautam, A. K. (2018). Mutual coupling reduction between elements of UWB MIMO antenna using small size uniplanar EBG exhibiting multiple stop bands. *AEU - International Journal of Electronics and Communications, 93*, 32-38. https://doi.org/10.1016/j.aeue.2018.05.033

[12] Wu, W., Yuan, B., & Wu, A. (2018). A quad-element UWB-MIMO antenna with band-notch and reduced mutual coupling based on EBG structures. *International Journal of Antennas and Propagation*. https://doi.org/10.1155/2018/8490740

[13] Orhan, A. & Mesud, K., (2022). The Effect of the Co-Planar Structure on HPBW and the Directional Gain at the Square Patch Antenna around ISM 2450 MHz. *Technical Gazette, 29*(4), 1120-1125. https://doi.org/10.17559/TV-20190423010908

[14] Kareemulla, S. & Kumar, V. (2022). Compact MIMO-Antenna with Enhanced Isolation for Ultra-Wide-Band and Ku-Band Applications. *Journal of Communications Technology and Electronics, 67*(1), 56-62. https://doi.org/10.1134/S1064226922010053

[15] Nguyen, T. T., Nghi, H. T., & Tutku K. (2022). Dual polarized patch antenna array with improved isolation and gain for full-duplex wireless communications. *Analog Integrated Circuits and Signal Processing, 112*(3), 475-484. https://doi.org/10.1007/s10470-022-02067-2

[16] Zhang, J., Xiuping, L., Zihang, Q., Yuhan, H., & Hua Z. (2022). Dual-Band Dual-Polarization Horn Antenna Array Based on Orthomode Transducers with High Isolation for Satellite Communication. *IEEE Transactions on Antennas and Propagation, 70*(10), 9247-9259. https://doi.org/10.1109/TAP.2022.3177473

[17] Sun, D. & Wei, C. (2016). Analysis and design of 4 × 4 MIMO-antenna systems in mobile phone. *Journal of Computer and Communications*, 26-33. https://doi.org/10.4236/jcc.2016.42004

[18] Kumari, T., Das, G., Sharma, A., & R. Kumar. (2018). Design approach for dual element hybrid MIMO antenna arrangement for wideband applications. *International Journal of RF Microwave Computer Aided Engineering*, 1-10. https://doi.org/10.1002/mmce.21486

[19] Wang, Z., Zhao, L., Cai, Y., Zheng, S., & Yin, Y. (2018). A Meta-surface Antenna Array Decoupling (MAAD) method for mutual coupling reduction in a MIMO antenna system. *Scientific Reports,* 1-9. https://doi.org/10.1038/s41598-018-21619-z

[20] Nandi, S. & Mohan, A. (2017). CRLH unit cell loaded triband compact MIMO antenna for WLAN/WIMAX applications. *IEEE Antennas Wireless Propagation Letters, 16*, 1816-1819. https://doi.org/10.1109/LAWP.2017.2681178

[21] Rao, P. S., Babu, K. J., & Prasad, A. M. (2017). Compact multi-band MIMO antenna with improved isolation. *Progress In Electromagnetics Research, 62*, 199-210. https://doi.org/10.2528/PIERM1709020101

[22] Ojaroudi Parchin, N., Jahanbakhsh Basherlou, H., Al-Yasir, Y. I., Ullah, A., Abd-Alhameed, R. A., & Noras, J. M. (2019). Multi-band MIMO antenna design with user-impact investigation for 4G and 5G mobile terminals. *Sensors, 19*, 456. https://doi.org/10.3390/s19030456

[23] Ikram, M., Nguyen-Trong, N., & Abbosh, A. (2019). Multiband MIMO microwave and millimeter antenna system employing dual-function tapered slot structure. *IEEE Transaction on Antennas Propagation, 67*, 5705-5710. https://doi.org/10.1109/TAP.2019.2922547

[24] Wang, H., Zhang, R., Luo, Y., & Yang, G. (2020). Compact eight-element antenna array for triple-band MIMO operation in 5G mobile terminals. *IEEE Access, 8*, 19433-19449. https://doi.org/10.1109/ACCESS.2020.2967651

[25] Islam, S. N. & Das, S. (2020). Dual-band cpw fed MIMO antenna with polarization diversity and improved gain.

International Journal of. RF Microwave and Computer-Aided Engineering, 30, e22128. https://doi.org/10.1002/mmce.22128

[26] Nguyen, N. L. (2019). Gain enhancement in MIMO antennas using defected ground structure. *Progress In Electromagnetics Research, 87*, 127-136. https://doi.org/10.2528/PIERM19091102

[27] Andrade, E. F., Miguel, A. P., Villanueva, R. G., & Aguilar, H. J. (2020). Characteristic mode analysis applied to reduce the mutual coupling of a four-element patch MIMO antenna using a defected ground structure. *IET Microwave Antennas Propagation, 14*, 215-226. https://doi.org/10.1049/iet-map.2019.0570

[28] Mark, R., Rajak, N., Mandal, K., & Das, S. (2019). Isolation and gain enhancement using metamaterial-based superstrate for MIMO applications. *Radio engineering, 28*, 689-695. https://doi.org/10.13164/re.2019.0689

Contact information:

R. SUDHA, Mrs., Assistant Professor
(Corresponding author)
Department of Electronics and Communication Engineering,
Sri Shakthi Institute of Engineering and Technology, India
E-mail: sudharamasamy@myyahoo.com

S. BHAVANI, PhD, Professor and Head
Department of Electronics and Communication Engineering,
Sri Shakthi Institute of Engineering and Technology, India
E-mail: bhavanisridharan7@gmail.com